

Draft - Submitted to *Journal of the Electrochemical Society*

Corrosion Behavior of a Novel SiC/Al₂O₃/Al Composite
Exposed To Chloride Environments

D.G. Kolman and D.P. Butt

Materials Corrosion and Environmental Effects Laboratory
Los Alamos National Laboratory
Los Alamos, NM 87545

Abstract

The electrochemical behavior of a new class of aluminum metal matrix composites produced by the direct metal oxidation technique, Lanxide AS-109™, was detailed. The composite is 69% (by volume) SiC reinforcement, 24% oxidized metal (primarily Al₂O₃), and 7% retained aluminum alloy. The corrosion behavior of the SiC/Al₂O₃/Al composite was found to be dependent on NaCl concentration and pH. SiC/Al₂O₃/Al was susceptible to pitting of the Al alloy phase at open circuit during exposure to aerated and deaerated 0.6, 0.06, and 0.006 M NaCl solutions. In contrast, exposure to 6x10⁻⁴ M NaCl did not result in pitting at open circuit, and buffered borate solution (no chloride) did not yield pitting at any potential examined. The pitting potential of SiC/Al₂O₃/Al was estimated to decrease 80 mV per order of magnitude increase in NaCl concentration. Comparison of the composite to a model composite matrix material, Al 6061, revealed that the composite was more susceptible to localized corrosion than the matrix alloy alone which did not pit at open circuit in deaerated 0.6 M NaCl. Polarization resistance measurements in pH adjusted (1 - 13) 0.6 M NaCl solutions revealed that the corrosion rate is minimized in neutral solution. Pits were neither confined to regions adjacent to SiC nor Al₂O₃, suggesting little galvanic effect of the reinforcing phases.

Introduction

Aluminum metal matrix composites (MMCs) are attractive for a wide variety of aerospace and defense applications because of their low density and their improved mechanical properties as compared to monolithic alloys. The corrosion behavior of this class of materials during exposure to chloride-containing environments has been studied by a variety of researchers.¹⁻¹³ Matrix materials of these composites can be comprised of either commercially pure aluminum^{1,2} or aluminum alloy²⁻¹², and the reinforcements are typically SiC¹⁻¹², Al₂O₃^{1,4}, or graphite^{2,7}. The aluminum MMCs that have been subjected to electrochemical testing have been produced in a wide variety of manners including hot pressing and/or extrusion^{1,5,6,9,10,11,12}, diffusion bonding^{2,7,13}, and casting^{4,8}. It is these variations in composition and processing which gives rise to often contradictory conclusions between studies.

Results from electrochemical testing of aluminum MMCs appear to be matrix alloy and processing dependent, given the different results stated in the literature. Perhaps the most controversial issue is the origin of the localized attack observed following exposure of aluminum MMCs to chloride environments. With few exceptions¹², localized attack occurs preferentially at the reinforcement/matrix interface^{1,3,4,7,8,9,10,13}. Attack at the interface has been attributed to galvanic corrosion between the reinforcement and matrix^{1,2,4}, crevice corrosion initiated at voids at the interface formed during processing^{3,4,9,11}, formation of intermetallic compounds that are more susceptible to pitting than the bulk matrix and that can preferentially form in the vicinity of the interface^{3,8,9,10,12}, and a defective passive film at the interface⁹ which arises from differences in the passive films formed on the different underlying materials¹⁴. Inherent to this controversy is the role of the reinforcement in the electrochemical behavior of aluminum MMCs. Conflicting results indicate that SiC is electrochemically active^{1,2,4} (i.e., able to participate in galvanic corrosion) and inert^{3,7,9}. This controversy may be due in part to the wide range of conductivities possible for SiC (10^{-5} - 10^{13} Ω -cm, as reported by Hihara and Latanison²), depending on its purity. The difficulty

in discerning the electrochemical effect of SiC arises from the fact that crevicing^{3,4,9,11}, due to defects in processing at an inert reinforcement interface with the matrix, cannot be discerned from galvanic corrosion effects at an electrochemically active reinforcement interface by visual observation.

The effect of reinforcement incorporation on values for nearly every pertinent parameter is unclear. For instance, there is controversy over whether the presence of the SiC reinforcement increases the pitting susceptibility (i.e., decreases the pit initiation potential (E_{pit}) or the repassivation potential (E_{rp}))^{5,10,15}, decreases the susceptibility^{4,7,8}, or has no effect^{1,3,5}. Corrosion current density has been shown to increase^{1,3,4,5,13}, decrease^{5,15}, and remain unaffected¹ in the presence of reinforcements. Additionally, reinforcements have been shown to increase^{1,5}, decrease^{5,10,13,15}, and not affect^{3,4,6,7} the open circuit potential (OCP). Other contrary results exist over the effect of the fraction of reinforcement^{1,2,4,6,8,13} and the pit size and morphology^{1,4,5,7,12}. The conflicting results are likely explained by differences in processing and composition which yield dramatically different electrochemical behavior. This explanation is reasonable because some of the contradictory results arise from within individual studies that incorporate different composites. Therefore, the corrosion behavior of new aluminum MMCs cannot be inferred from the studies of different MMCs in the literature and must be determined via laboratory testing.

Historically, electrochemical tests have incorporated aluminum MMCs prepared via conventional processing. However, a new class of composite materials is currently being produced via the direct metal oxidation (DIMOX) technique^{16,17,18}. In this technique, composites are formed via infiltration of a reinforcement preform with molten metal which is subsequently oxidized^{16,17}. The resulting product is a ternary composite comprised of retained metal, its oxidation product, and the reinforcement. This technique allows tailoring of material properties including strength, fracture toughness, density, and electrical conductivity. One particular material of interest, DIMOX AS-109™, is primarily SiC reinforcement and contains only 5-10% retained

aluminum alloy which is well dispersed throughout the Al/Al₂O₃ matrix. The corrosion resistance of this new class of composite is unknown. Since the material microstructure and processing history are remarkably different from other aluminum MMCs which have been studied, it is likely that the corrosion properties are different also. For instance, "near-interface" material has often been observed to dissolve preferentially vs. "remotely disposed" matrix material in conventional aluminum MMCs^{1,3,4,7,8,9,10,13}. However, the retained Al phase in this composite can be considered entirely "near-interface" material because it is small (1 - 50 μm). Thus, the deleterious effects of both the primary reinforcement (SiC) and the dual-phase matrix (comprised of retained metal and a secondary Al₂O₃ reinforcement) should be exacerbated. Also, because the areas of retained alloy are small and surrounded by SiC and Al₂O₃, metal dissolution is likely to result in the formation of a localized chemistry. This should also reduce the corrosion resistance of the composite. Therefore, the objective of this study is to detail the electrochemical behavior of a new class of SiC/Al₂O₃/Al composite exposed to chloride environments in order to detail the corrosion behavior in a variety of environments, examine the effects of pertinent environmental variables such as chloride concentration and solution pH, understand the underlying mechanisms which yield the observed behavior, and to discern the role of the reinforcements, if any. Electrochemical testing of this material is required in light of the dependence of corrosion properties on composite composition and processing history. Additionally, this work seeks to examine the electrochemical corrosion behavior of a ternary composite as well as a composite that is almost entirely comprised of ceramic, neither of which have been well characterized in the literature.

Experimental Procedure

Materials

The SiC/Al₂O₃/Al composite used for this study was Lanxide AS-109™, which is produced by the direct metal oxidation process^{16,17,18}. The material microstructure is shown in Figure 1a. The composite is considered to be an aluminum alloy / Al₂O₃ matrix composite reinforced with SiC particles. The nominal composition of the composite is 65% SiC (by volume), 25-30% Al₂O₃, and 5-10% retained aluminum alloy. Results of chemical composition measurements of the composite are displayed in Table 1. The estimated phase fraction of the composite, based on the elemental composition in Table 1, is shown in Table 2. Using a variety of techniques, the retained aluminum metal was estimated to be Al - >1 Si - 1 Fe - 0.7 Cu - 0.4 Mg (wt%). The precise concentration of Si in the retained Al was not able to be determined due to corruption of the analysis by adjacent SiC phases. Analysis of the oxidized metal phase suggested that it was primarily Al₂O₃ and depleted of alloying elements as compared to the retained metal. Based on the compositional analysis, aluminum alloy 6061 (Al - 0.6 Si - 0.7 Fe - 0.3 Cu - 1 Mg (wt%)) was used as a model of the retained Al alloy for this study.

1-3 cm² area samples were mounted in epoxy for electrochemical testing. Samples were wet polished to 3 μm grit with diamond paste, followed by ultrasonic cleaning in a mixed hydrocarbon solution (100 ethanol : 1 methanol : 1 ethyl acetate : 1 methyl isobutyl ketone). Samples were examined following exposure to ensure that no crevicing occurred at the sample/epoxy interface.

Environments

All solutions were prepared with distilled water and reagent grade chemicals. A pH of 6.4 was measured for aerated 0.6 M NaCl. Some 0.6 M NaCl solutions were pH adjusted to pH 1 or pH 4 with HCl, or to pH 10 or pH 13 with NaOH. Therefore, these pH adjusted solutions are nominally, but not exactly, 0.6 M NaCl. Buffered borate solution (pH 7.4) was comprised of 0.5 M boric acid buffered with 0.05 M sodium borate. The oxygen concentrations for actively aerated and deaerated solutions (with ultra high purity Ar gas) were measured as 6.4 ppm and 0.06 ppm, respectively. Gases were introduced to solution by fine porosity gas dispersion tubes with flow rates of approximately 45 cm³/min (0.1 scfh). A solution volume of 500 ml was used for all tests.

Electrochemical Testing

Electrochemical measurements were performed with several different commercially available potentiostats under software control. All potentiodynamic scan rates were 0.05 mV/s. Samples were immersed in solution for 4 hours at open circuit (OC) preceding potentiodynamic polarization tests. OCP measurements over a one week period (aerated 0.6 M NaCl) indicated that the OCP of the SiC/Al₂O₃/Al composite at 4 hours was nearly identical (+/- 20 mV) to that at one week. Thus, polarization behavior following a 4 hour immersion is considered to be indicative of that at steady state. Electrochemical cells were composed of a glass five-neck flask, a platinized Nb counter electrode, and either a saturated calomel electrode (SCE) or a Hg/HgSO₄ electrode as a reference electrode. The Hg/HgSO₄ electrode was used with buffered borate solution to prevent chloride contamination. All potentials are referenced to the SCE. Polarization resistance measurements were conducted via potentiodynamic polarization and electrochemical impedance spectroscopy (EIS). Surface areas were not corrected for surface roughness. The entire exposed surface area of the SiC/Al₂O₃/Al composite was used for current density calculations (as opposed to the retained metal area alone). Thus, assuming that the SiC and Al₂O₃ phases are inert (see

Results and Discussion), the current densities for retained metal regions are approximately 14 times larger than that of the composite as a whole because the retained metal comprises approximately 1/14 of the composite surface area. Similarly, polarization resistances of the retained metal are actually 14 times smaller.

Data were not corrected for the inherent sample resistance which is negligible based on electrochemical impedance spectroscopy (EIS) measurements. EIS tests incorporated identical areas (1.74 cm^2) of SiC/Al₂O₃/Al (0.5 cm thick) and 304 stainless steel (SS) individually exposed to an identical solution (aerated 0.6 M NaCl). The measured impedance spectrum is displayed in Figure 2. Assuming a negligible material resistance for the SS sample, the high frequency impedance approach to the Z' axis (real component of the impedance) corresponds to the solution resistance. Since the solution resistance for the SS and SiC/Al₂O₃/Al samples are identical for specimens of identical geometry and fixed cell geometry, the solution resistance obtained from the SS test may be subtracted from the high frequency impedance of the SiC/Al₂O₃/Al sample to yield an estimate of the sample resistance. Using this approach, the sample resistance was calculated to be 2.6Ω . The material resistance is considered to be negligible for the present study. Therefore, data were not adjusted for potential drop within the material.

Results and Discussion

Anodic and Cathodic Reactions Determining the Open Circuit Potential in Neutral Environments

Polarization curves for aerated 0.6 M NaCl, deaerated 0.6 M NaCl and buffered borate solution are shown in Figure 3. The corrosion current densities of SiC/Al₂O₃/Al samples exposed to the deaerated environments of Figure 3 are lower than that of the aerated solution. This is

explained by the cathodic polarization data. The cathodic branches of the aerated and deaerated solution are controlled by mass transport limitation, almost certainly oxygen reduction. Thus, the corrosion current density is determined almost entirely by the cathodic reaction rate since the cathodic slope is nearly infinite on the $E - \log i$ plot while the anodic slope is practically zero. Because the cathodic current density is proportional to the dissolved oxygen concentration, and because the corrosion current density is practically equivalent to the cathodic current density, a roughly two orders of magnitude increase in the dissolved oxygen concentration should yield a two orders of magnitude increase in corrosion current density. Indeed, polarization resistance measurements indicated a 2-3 orders of magnitude increase in the corrosion rate in aerated 0.6 M NaCl, as compared to deaerated 0.6 M NaCl, which corresponds well with the two orders of magnitude increase in dissolved oxygen concentration. Therefore, the cathodic reaction rate is shown to control the corrosion rate of SiC/Al₂O₃/Al in 0.6 M NaCl.

The anodic kinetics are more complex. In buffered borate solution, the SiC/Al₂O₃/Al sample is passive over the entire measured anodic potential range. In contrast, SiC/Al₂O₃/Al does not reveal a passive region when exposed to 0.6 M NaCl. For the 0.6 M NaCl solutions, the slope of the anodic branch is shallow (approximately 20 mV/decade), and the anodic kinetics are independent of aeration level (i.e., the aerated and deaerated curves overlies one another).

Figure 4 shows anodic polarization data for SiC/Al₂O₃/Al exposed to deaerated 0.6 M NaCl. No trend of composite polarization resistance with chloride concentration was observed for all of the deaerated chloride solutions (all were approximately 10⁶ Ω-cm²). This supports the prior assertion that the corrosion current density is cathodic reaction rate controlled in these environments, because the variations in chloride concentration alter the anodic kinetics. Therefore, the corrosion current density can be maintained at a relatively low value in 0.6 M NaCl if the dissolved oxygen concentration can be kept to a minimum. Note that the corrosion current density

is an average current density (total current / composite surface area) and does not represent the local anodic current densities within the pits which are actually much larger.

The anodic reaction on SiC/Al₂O₃/Al appears to be controlled by pitting of the aluminum metal, as evidenced in Figure 4. The anodic behaviors during exposure to deaerated 0.006 M, 0.06 M, and 0.6 M NaCl are similar, each exhibiting pitting at OC. In contrast, SiC/Al₂O₃/Al is spontaneously passive (i.e., no pitting was observed) at OC in deaerated 6x10⁻⁴ M NaCl. Upon anodic polarization of a few hundred mV in deaerated 6x10⁻⁴ M NaCl, a pitting potential is revealed. Since pitting is observed at 6x10⁻⁴ M NaCl, pitting will most certainly occur at higher NaCl concentrations, with the pitting potential decreasing with increasing NaCl concentration¹⁹. Thus, it is logical to assume that the pitting potential in the more concentrated solutions is below the OCP and cannot be observed. Indeed, pitting was observed following immersion in 0.6 M NaCl (see "Localized Corrosion" below). In summary, the mixed potentials for the 0.006, 0.06, and 0.6 M NaCl tests appear to be comprised of anodic pitting and cathodic oxygen reduction. In contrast, 6x10⁻⁴ M chloride promotes a mixed potential comprised of passive dissolution and cathodic oxygen reduction.

Localized corrosion of SiC/Al₂O₃/Al composite

Post-immersion microscopy confirmed that SiC/Al₂O₃/Al pits at OC. SiC/Al₂O₃/Al samples were immersed in 0.6 M NaCl for 4 hours (not shown), 26 hours (Figure 1b) and 168 hours (Figure 1c). Optical microscopy revealed no pitting following the 4 hour immersion even though polarization curves initiated following 4 hour immersion indicate that pitting occurs. The apparent discrepancy likely arises from the insensitivity of optical microscopy as compared to electrochemical testing. Conversely, the 26 hour test produced corrosion pits within regions of retained Al alloy. Not all retained alloy regions were pitted. Corrosion pits were less than 5 μm in depth following the 26 h immersion in 0.6 M NaCl. The 168 hour immersion produced more

severe damage, with entire pockets of retained aluminum alloy dissolved from within the inter-SiC matrix. These pits correspond to areas previously comprised of Al alloy. A random sample of 50 pits indicated penetration depths ranging from 4.5 μm to 69 μm following the 168 hour exposure to 0.6 M NaCl. The distribution of pit sizes is shown in Figure 5.

The pit nucleation potential for aluminum can be described by the equation

$$E_{\text{pit}} = A - B \log [\text{Cl}^-]$$

where B has been shown to vary between 50 and 130 mV ($0.01 \text{ M} < [\text{Cl}^-] < 5 \text{ M}$).¹⁹ B can be estimated using E_{tp} , the potential at which the anodic scan crosses itself on the return scan (not shown). Over the 0.006 to 0.6 M range, B was found to be 73 mV, which is in good agreement with the literature values.¹⁹ The value of A was $-0.890 V_{\text{SCE}}$. Moreover, assuming that the cathodic current density (oxygen reduction rate) is independent of potential between $-0.7V_{\text{SCE}}$ and $-1V_{\text{SCE}}$, the OCP can be used as a reasonable approximation of E_{pit} . Using OCP in place of E_{pit} , a B of 83 mV is obtained over the 0.006 to 0.6 M range. This agrees with the B obtained using E_{tp} as well as that observed elsewhere¹⁹. The value of A was $-0.938 V_{\text{SCE}}$.

Corrosion pits appeared to be homogeneously distributed throughout the matrix following a one week immersion in 0.6 M NaCl. That is, the pits were not solely confined to regions immediately adjacent to SiC or Al_2O_3 . If there is some galvanic interaction between the retained metal and the SiC and Al_2O_3 phases, neither the SiC nor the Al_2O_3 appears to have a greater effect on galvanic corrosion. However, Al_2O_3 is unlikely to interact galvanically with the retained Al alloy because Al_2O_3 is an insulator. Thus, it seems unlikely that galvanic effects play a significant role in metal dissolution given that neither phase appears to preferentially promote localized corrosion and that galvanic interaction with Al_2O_3 is likely to be insignificant.

Comparison of SiC/Al₂O₃/Al Composite Behavior to that of Monolithic Model Matrix Material

The anodic polarization behavior of the SiC/Al₂O₃/Al composite exposed to deaerated 0.6 M NaCl is compared to that of Al 6061 in Figure 6. Al 6061 is considered to roughly simulate the composition of the retained metal in the MMC (see Experimental Procedure). Thus, a comparison of the corrosion behavior of the two materials provides insight into the effect of the processing history and reinforcements on the electrochemical behavior of the MMC.

The presence of the reinforcement is deleterious to the localized corrosion resistance of the SiC/Al₂O₃/Al composite. The MMC pits at its OCP in deaerated 0.6 M NaCl whereas Al 6061 does not. The MMC is less resistant to pitting as evidenced by the more negative pitting potential, $-0.93V_{SCE}$ for the MMC vs. $-0.74V_{SCE}$ for Al 6061. (The pitting potential for Al 6061 agrees well with other published results for Al 6061 exposed to deaerated 0.6 M NaCl.^{2,3}) Additionally, the OCP of the MMC is more positive than that of Al 6061. The more positive pitting potential and more negative OCP of the MMC results in a reduced driving force required for pitting. That is, the anodic overpotential required for pitting in deaerated 0.6 M NaCl is approximately 0.26V for Al 6061 as compared to 0V for the MMC. The decrease in driving force required for localized corrosion of the MMC is likely attributable to the introduction of reinforcement/matrix interfaces which have been shown to enhance localized corrosion^{1,3,4,7,8,9,10,13} and the MMC microstructure which contains a fine distribution of retained metal that is all near-interface material. Because the alloy regions are all near-interface material (i.e., the retained alloy regions are small), all of the alloy material is bounded by areas which do not dissolve. Thus, a localized solution chemistry is more likely to develop in the MMC than the monolithic alloy because dissolution results in a recessed alloy surface.

The polarization resistance of the retained Al alloy within the MMC can be calculated and compared to that of Al 6061 if it is assumed that all of the anodic current results from anodic

reactions on the retained Al alloy alone. The polarization resistance of the retained metal phase alone is calculated by multiplying the MMC polarization resistance ($1.2 \times 10^6 \Omega\text{-cm}^2$) by the surface area fraction of retained alloy, 0.073, assuming that the fraction is unchanged during immersion. A polarization curve normalized for retained Al alloy area is shown in Figure 6. The polarization resistance of the retained metal ($8 \times 10^4 \Omega\text{-cm}^2$) was found to be larger than that of Al 6061 ($3 \times 10^4 \Omega\text{-cm}^2$). Thus, the corrosion current density is actually smaller. Note that differences between the corrosion current densities these values may be insignificant given the uncertainty in surface area. Regardless, no dramatic difference (i.e., an order of magnitude or more) between the corrosion current densities is observed. Therefore, the presence of the SiC and Al_2O_3 reinforcements is not deleterious to the overall or average corrosion current density. This result is consistent with the prior assertion that the corrosion current density is oxygen reduction rate (or oxygen concentration) controlled. However, because the corrosion current density represents an average current density, the MMC will exhibit a larger maximum penetration because the anodic current is localized to small regions of intense dissolution. So the presence of the reinforcements is detrimental to the corrosion resistance of the composite even though its average corrosion rate is similar to that of Al 6061. In summary, the combination of reinforcement inclusion and processing history increases the susceptibility of SiC/ Al_2O_3 /Al to pitting by reducing the driving force required for pitting (i.e., lowering the pitting potential and increasing the OCP). This reduction in driving force results in localized corrosion of the MMC at OC, in contrast to the monolithic Al alloy material. However, the retained alloy corrosion current density is not increased by the presence of inclusions and the processing history of the MMC.

Effect of pH on Corrosion in 0.6 M NaCl Solutions

The effect of pH on the electrochemical behavior of SiC/ Al_2O_3 /Al exposed to chloride solution was examined. Anodic polarization curves for pH 1, 4, 6.4 (nonadjusted), 10 and 13 are shown in Figure 7. All solutions promoted pitting at OC. Anodic behavior in the near-neutral

solutions (pH 4 and 10) is nearly identical to that in neutral solution, resulting in similar OCPs and corrosion current densities. Since the OCPs roughly approximate the pitting potential here, the results are in agreement with literature discussions which state that the pitting potential is independent of pH over this pH range.^{20,21} The OCPs of SiC/Al₂O₃/Al exposed to both pH 1 and pH 13 solutions are different from those in neutral and near-neutral solutions. This difference arises from changes in both the anodic kinetics (Figure 7) and cathodic kinetics. In contrast to the mixed potential in neutral solution, which is determined by anodic pitting and oxygen reduction, the mixed potentials generated by pH 1 and pH 13 solutions are composed of anodic pitting and hydrogen evolution (Figure 8). Further, the polarization resistance was found to be a maximum at neutral pH (Figure 9). This is consistent with the minimum in corrosion rate of Al in neutral solutions observed in a wide variety of environments.²² Therefore, the corrosion rate can be controlled by varying the solution pH.

Although it seemed apparent from microscopy following different immersion periods that corrosion pits resulted from Al alloy dissolution, it could be argued that the observed pits are attributable to phase "fall-out". However, the following experimental results support the assertion that corrosion pits originate from Al alloy dissolution. A white precipitate was noted in solution following anodic polarization tests on SiC/Al₂O₃/Al in neutral and near-neutral chloride solutions. No precipitate was observed following testing in buffered borate solution, 0.6 M NaCl adjusted to pH 1, or 0.6 M NaCl adjusted to pH 13. Following immersion of SiC/Al₂O₃/Al in 0.6 M NaCl, the precipitate was filtered from solution and allowed to dry. X-ray diffraction analysis of the precipitate indicated that the compound was aluminum hydroxide containing a small percentage of Al₂O₃. Integration of the anodic data indicated that the anodic charge passed during the borate test (0.012 C) was much lower than that passed during any neutral chloride test (11 C (6x10⁻⁴ M NaCl) - 280 C (0.6 M NaCl)). Assuming a dissolution valence of 3, the aluminum concentration in the buffered borate was calculated to be 8 x 10⁻⁸ M, which is below the experimentally determined solubility limit of approximately 10⁻⁵ M in near-neutral solution²³. The aluminum concentration in

the neutral chloride solutions was between 8×10^{-5} M and 2×10^{-3} M, which exceeds the solubility limit in neutral solutions and results in precipitation. The lack of precipitation in the strongly alkaline and acidic chloride solutions is attributable to the fact that the aluminum concentrations are similar to those in neutral solution but that the solubility limits are much larger at the pH extrema (10^7 - 10^{11} times larger than that in neutral solution)²⁴. Thus, the observed precipitation (or lack of precipitation) in every solution examined can be explained by comparison of solution concentration calculated from anodic data with the corresponding aluminum solubility limit. Therefore, the presence of oxidized aluminum compounds provides independent confirmation that the Al phase is dissolved upon anodic polarization of the SiC/Al₂O₃/Al composite exposed to 0.6 M NaCl solutions.

Conclusions

The corrosion behavior of a SiC/Al₂O₃/Al composite exposed to chloride solutions was examined. The mixed potential in neutral and near-neutral chloride solutions was determined by anodic pitting of the retained Al alloy phase and cathodic oxygen reduction. One exception to this was 6×10^{-4} M NaCl solution which promoted passivity at OC. The pitting potential of SiC/Al₂O₃/Al decreased by 80 mV per order of magnitude increase in NaCl concentration. Both post-immersion microscopy and solution precipitate analysis revealed that the corrosion pits resulted from dissolution of the retained Al phase. Corrosion pits within the retained alloy phase were observed following 26 hour immersion in 0.6 M NaCl. Pits within the retained alloy were not observed following a 168 hour immersion. Rather, entire regions of the finely dispersed Al alloy phase were dissolved.

The electrochemical behavior of the MMC was compared to that of Al 6061. Al 6061 roughly approximates the composition of the retained metal phase in the MMC. In contrast to

SiC/Al₂O₃/Al composite, Al 6061 did not pit at OC in deaerated 0.6 M NaCl. The MMC had a more positive OCP and a more negative pitting potential than Al 6061. Thus, the MMC required a smaller driving force for pitting (0V) than the model monolithic matrix material (0.26V). Therefore, the presence of the reinforcements and/or the processing of the MMC is deleterious to the localized corrosion resistance. However, the overall corrosion current density of the MMC was not higher than that of the monolithic material as a result of cathodic oxygen reduction control of the corrosion rate.

The effect of solution pH (pH 1 - 13) on the corrosion of SiC/Al₂O₃/Al exposed to 0.6 M NaCl was examined. Polarization resistance measurements indicated that the corrosion rate is minimized at intermediate (neutral) pH. Pitting was observed at OC regardless of solution pH. At pH extrema (pH 1 and 13), both the anodic and cathodic kinetics were significantly different from those in neutral 0.6 M NaCl. The cathodic reaction is controlled by hydrogen evolution during immersion of SiC/Al₂O₃/Al in pH 1 and 13 NaCl solutions, as opposed to oxygen reduction at intermediate pH. Anodic dissolution resulted in precipitation of an aluminum hydroxide compound in neutral and near-neutral NaCl solutions but not in pH 1 and 13 solutions due the higher solubility of aluminum hydroxide at the pH extrema.

References

- 1) C. Monticelli, F. Zucchi, F. Bonollo, G. Brunoro, A. Frignani, and G. Trabaneli, *J. Electrochem. Soc.*, **142**, 405 (1995).
- 2) L.H. Hihara and R.M. Latanision, *Corrosion*, **48**, 546 (1992).
- 3) W.N.C. Garrard, *Corrosion Science*, **36**, 837 (1994).
- 4) P.C.R. Nunes and L.V. Ramanathan, *Corrosion*, **51**, 610 (1995).
- 5) P.P. Trzaskoma, E. McCafferty and C.R. Crowe, *J. Electrochem. Soc.*, **130**, 1804 (1983).
- 6) H. Sun, E.Y. Koo, and H.G. Wheat, *Corrosion*, **47**, 741 (1991).
- 7) D.M. Aylor and P.J. Moran, *J. Electrochem. Soc.*, **132**, 1277 (1985).
- 8) M.M. Buarzaiga and S.J. Thorpe, *Corrosion*, **50**, 176 (1994).
- 9) J.E. Castle, L. Sun, and H. Yan, *Corrosion Science*, **36**, 1093 (1994).
- 10) J.F. McIntyre, R.K. Conrad, and S.L. Golledge, *Corrosion*, **46**, 902 (1990).
- 11) R.C. Paciej and V.S. Agarwala, *Corrosion*, **42**, 718 (1986).
- 12) P.P. Trzaskoma, *Corrosion*, **46**, 402 (1990).
- 13) A.J. Sedriks, J.A.S. Green, and D.L. Novak, *Met. Trans. A*, **2**, 871 (1971).
- 14) J. Kruger, R.S. Lillard, C.C. Streinz, and P.J. Moran, *Mater. Sci. Eng.*, **A198**, 11 (1995).
- 15) M.S.N. Bhat, M.K. Surappa, and H.V.S. Nayak, *J. Mater. Sci.*, **26**, 4991 (1991).
- 16) A.W. Urquhart, *Mater. Sci. Eng.*, **A144**, 75 (1991).
- 17) M.S. Newkirk, A.W. Urquhart, H.R. Zwicker, and E. Breval, *J. Mater. Res.*, **1**, 81 (1986).
- 18) M.K. Aghajanian, N.H. Macmillan, C.R. Kennedy, S.J. Luszcz, and R. Roy, *J. Mater. Sci.*, **24**, 658 (1989).
- 19) "Pitting Corrosion of Metals", Z. Szklarska-Smialowska, NACE, Houston, TX, p. 204 (1986).
- 20) W.J. Rudd and J.C. Scully, *Corrosion Science*, **20**, 611 (1980).
- 21) H. Böhni and H.H. Uhlig, *J. Electrochem. Soc.*, **116**, 906 (1969).
- 22) E.H. Hollingsworth and H.Y. Hunsicker in "ASM Handbook, Vol. 13, Corrosion", ASM International, Metals Park, OH, p. 608 (1992).
- 23) C. Edeleanu and U.R. Evans, *Trans. Faraday Soc.*, **47**, 1121 (1951).
- 24) "Atlas of Electrochemical Equilibria in Aqueous Solutions", M. Pourbaix, 2nd edition, NACE, Houston, TX (1974).

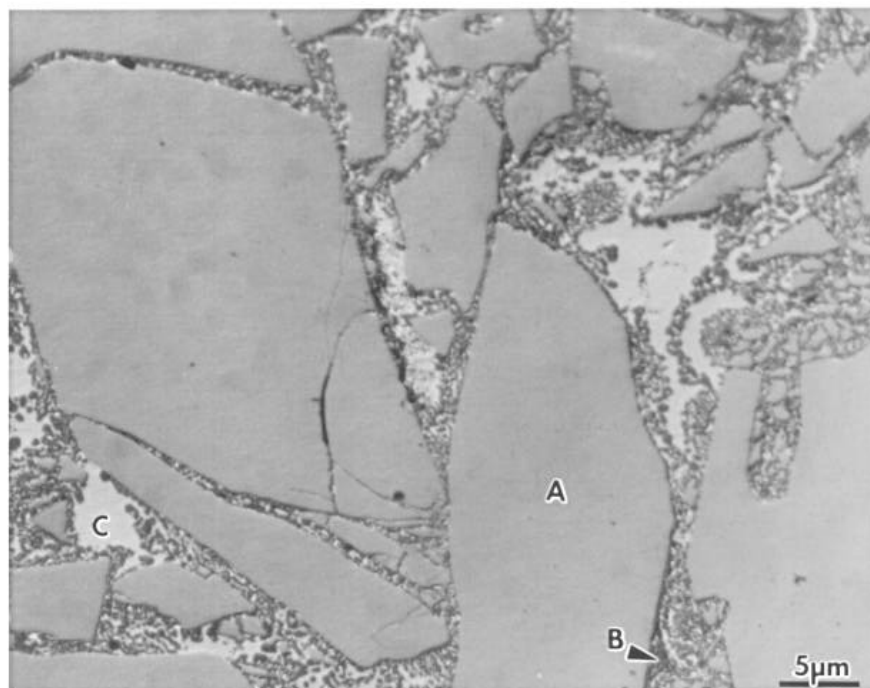
	Si	C	O	Al	Fe	Mg	Cu	Sn	Zn
atomic%	34.44	33.27	16.58	15.43	0.14	0.07	0.05	0.01	0.003
weight%	46.88	19.57	12.86	20.18	0.38	0.08	0.15	0.08	0.01

Table 1 - Elemental composition of the SiC/Al₂O₃/Al composite.

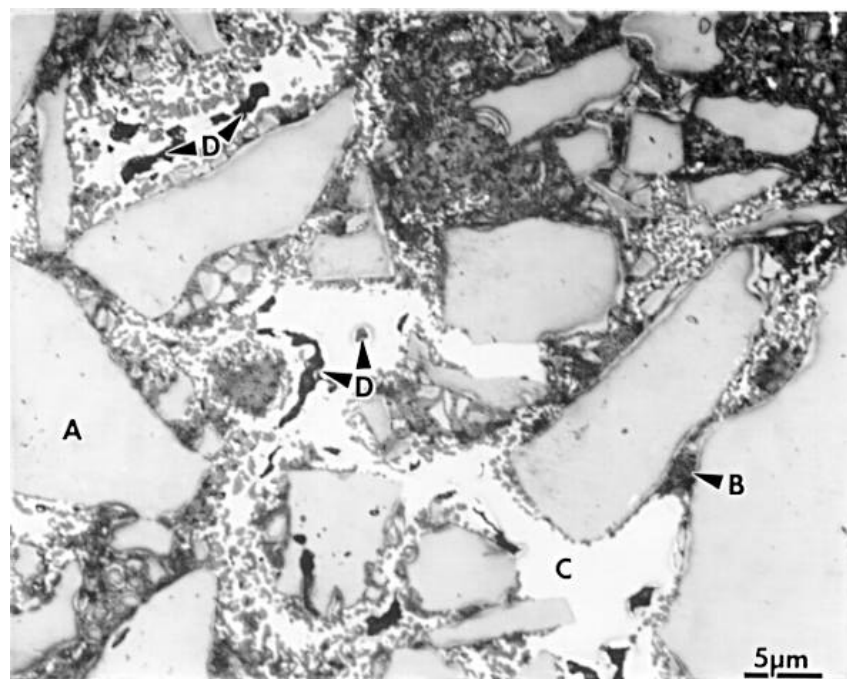
	SiC	Al ₂ O ₃	Retained metal
volume%	68.8	23.8	7.3
weight%	66.0	28.2	5.9

Table 2 - Estimated composition of the SiC/Al₂O₃/Al composite by phase.

a)



b)



c)

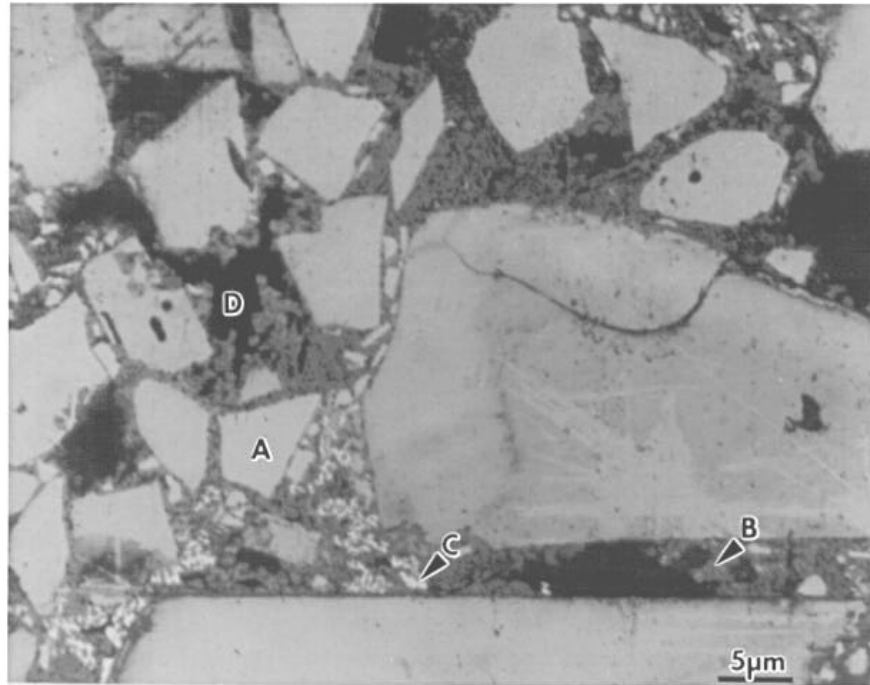


Figure 1 - Optical micrograph of SiC/Al₂O₃/Al microstructure. a) As polished, prior to immersion. b) Following a 26 h immersion in 0.6 M NaCl. c) Following a 168 h immersion in aerated 0.6 M NaCl. Marked areas are SiC (A), Al₂O₃ (B), retained aluminum alloy (C), and corrosion pits (D).

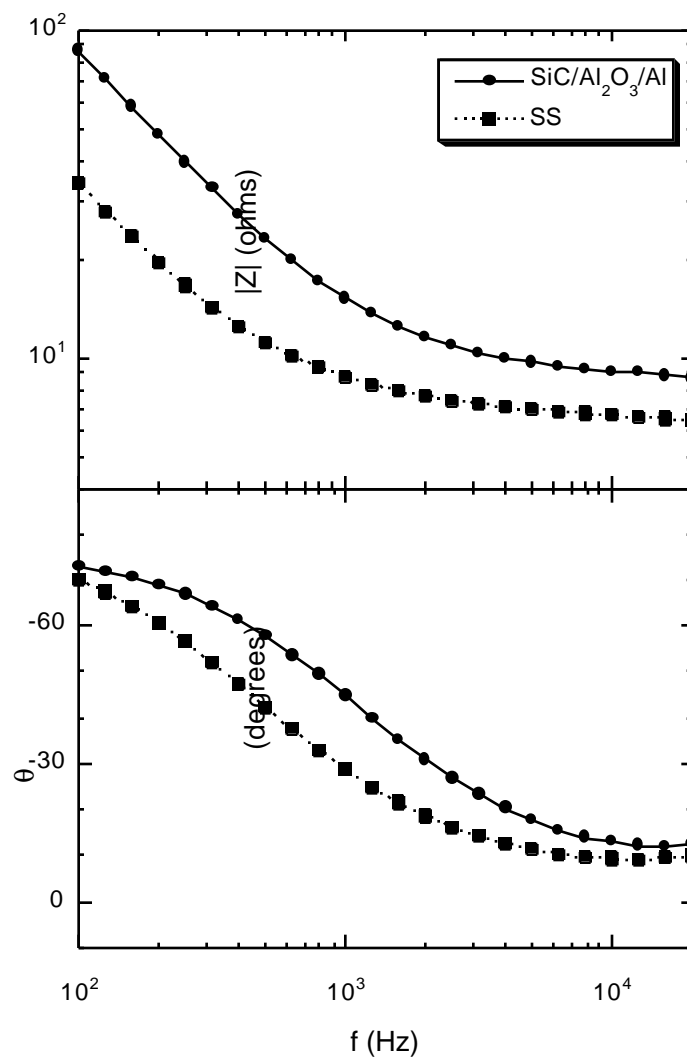


Figure 2 - Comparison of electrochemical impedance spectra of SiC/Al₂O₃/Al composite and 304 SS exposed to 0.6 M NaCl. The SiC/Al₂O₃/Al sample thickness was 0.5 cm.

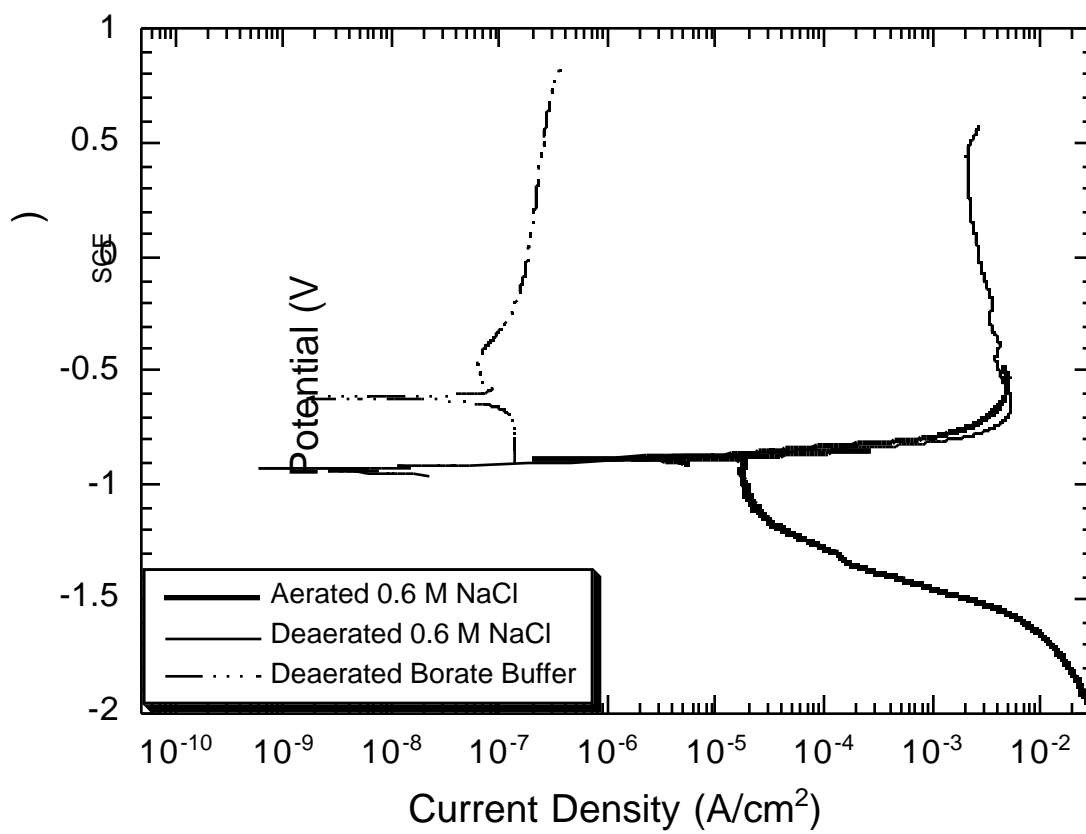


Figure 3 - Polarization curves on SiC/Al₂O₃/Al composite exposed to aerated 0.6 M NaCl, deaerated 0.6 M NaCl, and deaerated borate buffer.

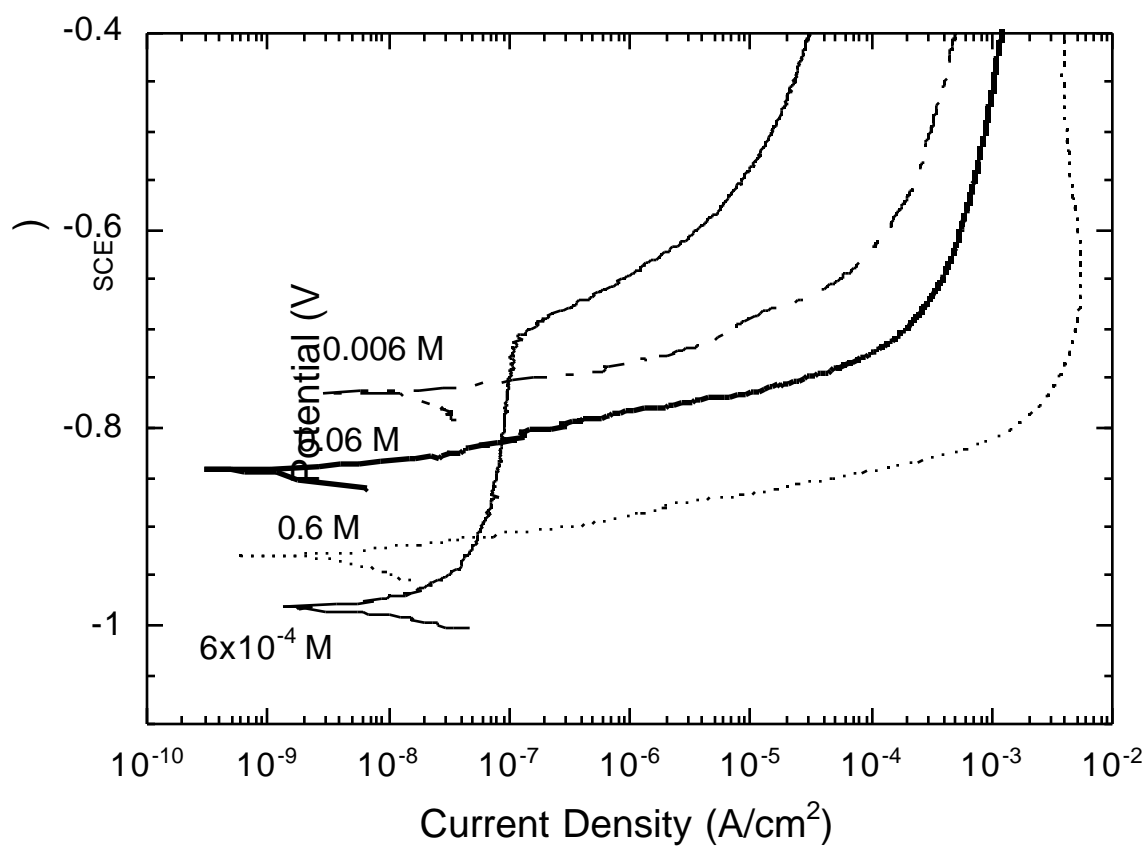


Figure 4 - Anodic polarization data from SiC/Al₂O₃/Al exposed to deaerated NaCl solutions of differing concentration.

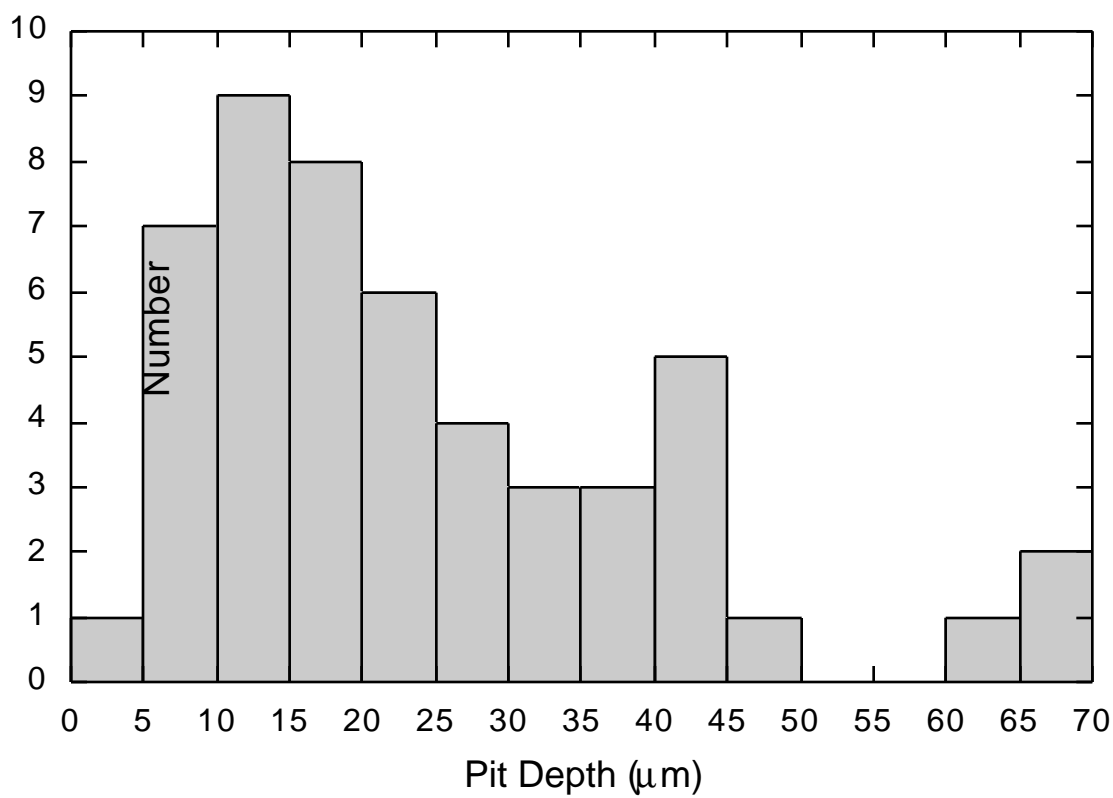


Figure 5 - Distribution of pits depths following one week exposure of SiC/Al₂O₃/Al to aerated 0.6 M NaCl.

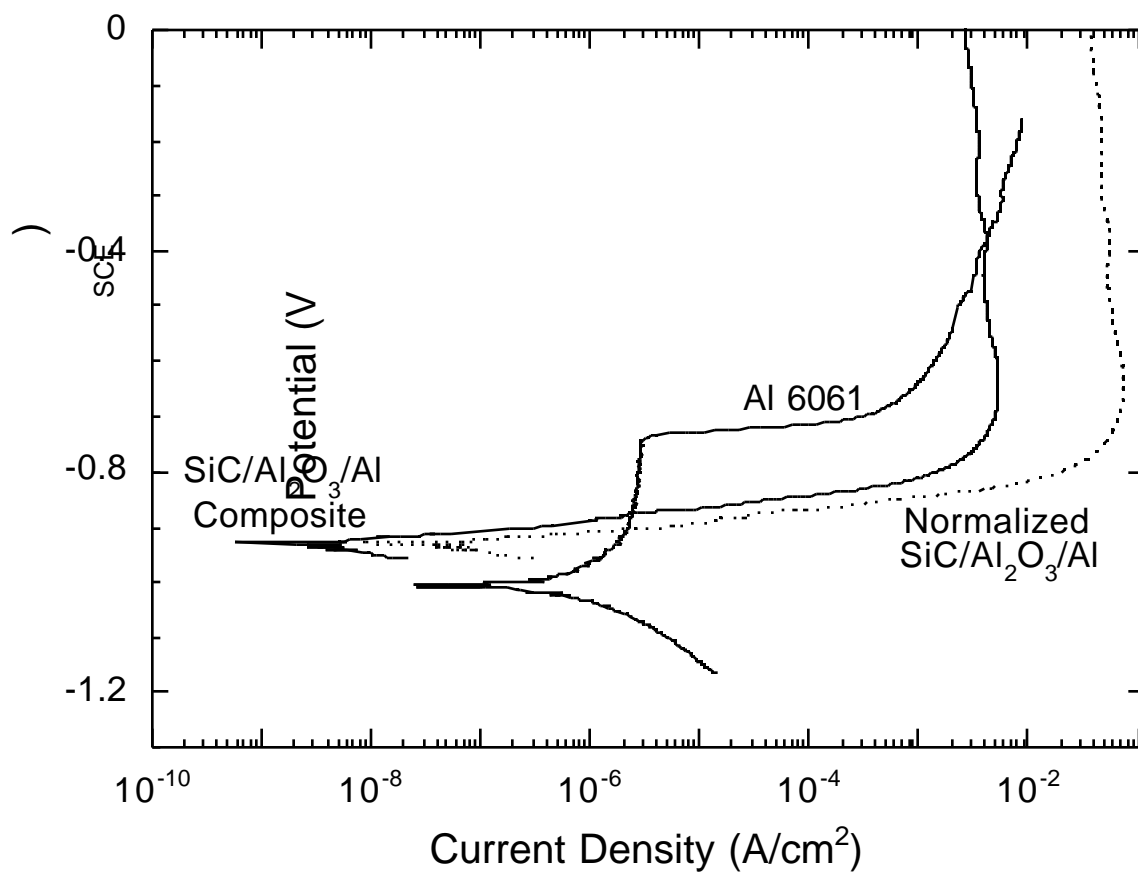


Figure 6 - Anodic polarization curves of SiC/Al₂O₃/Al, SiC/Al₂O₃/Al normalized for retained alloy area, and Al 6061 exposed to deaerated 0.6 M NaCl. Al 6061 roughly approximates the composition of the matrix material in SiC/Al₂O₃/Al.

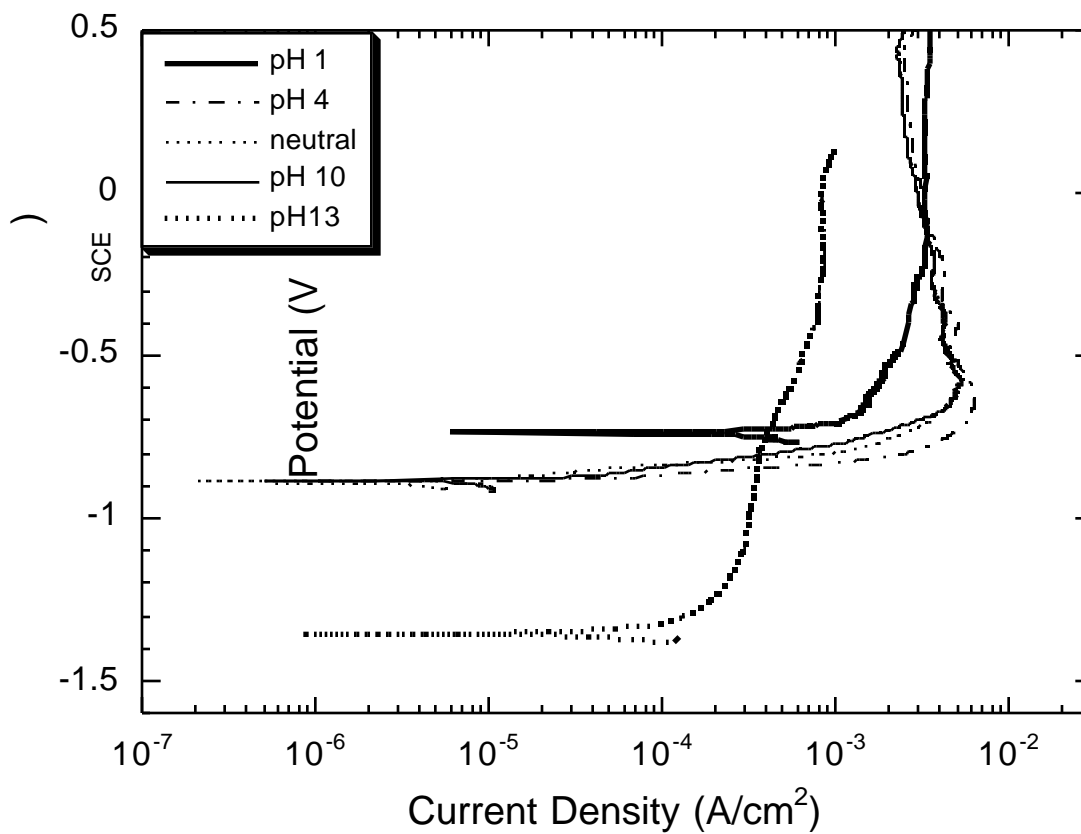


Figure 7 - Anodic polarization curves of SiC/Al₂O₃/Al exposed to aerated, nominally 0.6 M NaCl solutions of varying pH.

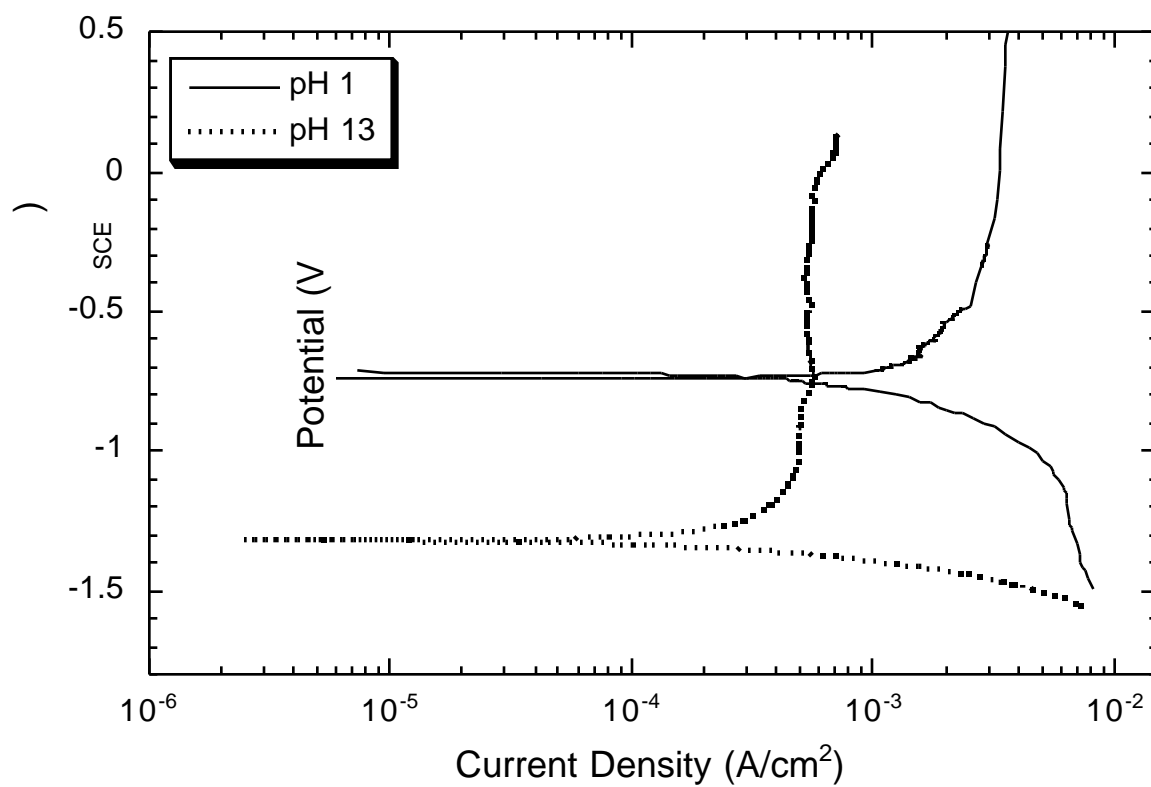


Figure 8 - Anodic and cathodic polarization data from SiC/Al₂O₃/Al exposed to aerated 0.6 M NaCl (nominal) adjusted to pH 1 and pH 13.

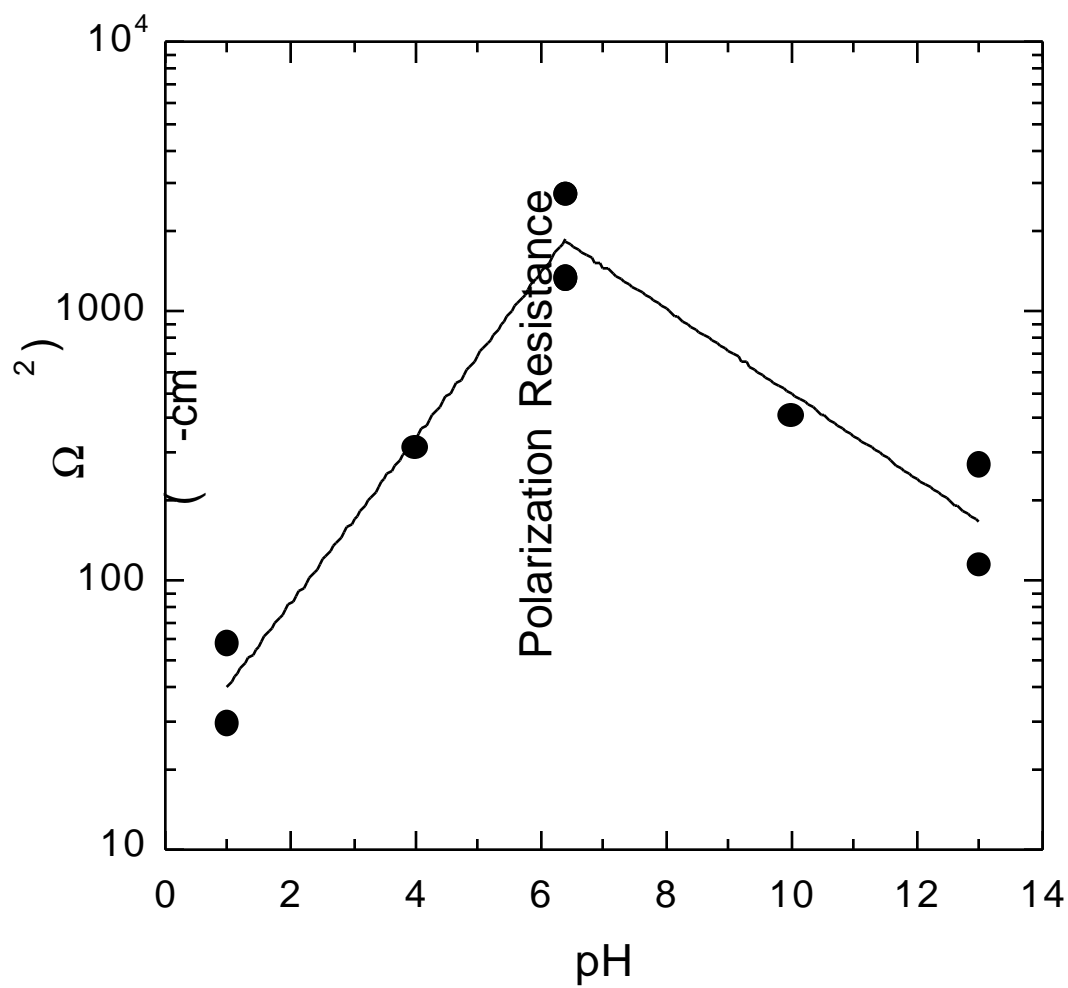


Figure 9 - Polarization resistances of SiC/Al₂O₃/Al exposed to aerated 0.6 M NaCl (nominal) as a function of pH.